Inorg. Chem. **2002**, *41*, 5286–5295

Synthesis and Characterization of a Series of (Hydroperoxo)-, (Alkylperoxo)-, and (μ-Peroxo)palladium Complexes Containing the Hydrotris(3,5-diisopropylpyrazolyl)borato Ligand (Tp^{iPr2}): (Tp^{iPr2})(py)Pd–OO–X [X = H, *t*-Bu, Pd(Tp^{iPr2})(py)] and (Tp^{iPr2})(py)Pd–(μ-κ^1:κ^2-OO)–PdTp^{iPr2}

Taichi Miyaji, Masato Kujime, Shiro Hikichi,[1] Yoshihiko Moro-oka, and Munetaka Akita*

Chemical Resources Laboratory, Tokyo Institute of Technology, 4259 Nagatsuta, Midori-ku, Yokohama 226-8503, Japan

Received May 20, 2002

Dehydrative condensation of the hydroxopalladium complex (Tp^{iPr2})(py)Pd–OH (**1**) with hydroperoxides (XOOH: X = H, *t*-Bu) produces the corresponding (hydroperoxo)-, (Tp^{iPr2})(py)Pd–OOH (**2a**), and (*tert*-butylperoxo)palladium complexes, (Tp^{iPr2})(py)Pd–OOBu^t (**3**). Treatment of **2a** with PPh_3 results in concomitant ligand displacement giving (Tp^{iPr2})(Ph_3P)Pd–OOH (**2b**) and oxygenation of PPh_3 giving O=PPh_3. Further condensation between **1** and **2a** gives the μ-κ^1:κ^1-peroxo complex (Tp^{iPr2})(py)Pd–OO–Pd(Tp^{iPr2})(py) (**4**), while condensation between the bis(μ-hydroxo)dipalladium complex ($PdTp^{iPr2}$)$_2$(μ-OH)$_2$ (**7**) with **2a** affords the unsymmetrical μ-κ^1:κ^2-peroxo complex (Tp^{iPr2})(py)Pd–OO–PdTp^{iPr2} (**5**). These peroxopalladium complexes **2**–**5** have been fully characterized by a combination of spectroscopic and crystallographic analyses, which lead to description of the O–O moieties in these complexes as peroxide (O_2^{2-}) with sp^3-hybridized oxygen atoms. The OOH moiety in **2b** is found to interact with the noncoordinated nitrogen atom of the pendant pyrazolyl group through hydrogen bond. The O_2 moieties in **2**–**5** turn out to be so nucleophilic (basic) as to add across carbon–heteroatom multiple bonds in acetonitrile and acetaldehyde to give the peroxometallacycle Tp^{iPr2}Pd[OOC(Me)=N)]Pd(Tp^{iPr2})(py) (**8**) (from **2**, **4**, and **5**) and the acetato complex (Tp^{iPr2})(py)Pd–OC(=O)CH_3 (**9**) (from **2**–**4**), respectively. Methyl vinyl ether and styrene, CH_2=CHY (Y = OMe, Ph), are converted to the corresponding methyl ketones, CH_3C(=O)Y, upon treatment with **2**–**4**.

Introduction

The chemistry of transition metal peroxo species has been an intensively studied subject in various fields of chemical research, because the transition metal−O_2 adducts play pivotal roles in various oxidative organic and biological transformations as well as O_2 transport in biological systems.[2] Detailed inorganic study of isolable O_2 complexes would provide valuable information on the structural and reaction aspects of O_2 activation and clues to elucidate the oxygenation mechanisms.

O_2 complexes have been usually prepared by oxidative addition of an O_2 molecule to a low-valent precursor.[3] In addition to this classical synthetic method dehydrative condensation of transition metal−hydroxo complex with H_2O_2 developed in our laboratory has been frequently utilized in recent synthetic studies of dinuclear peroxo complexes (Scheme 1).[4,5] This condensation method has advantages that (1) the method is applicable to the systems where an appropriate low-valent metal precursor is not available and

* To whom correspondence should be addressed. E-mail: makita@res.titech.ac.jp.

(1) Present address: Department of Applied Chemistry, School of Engineering, University of Tokyo, Hongo, Bunkyo-ku, Tokyo 113-8656, Japan.

(2) (a) Special thematic issue for "bioinorganic enzymology": *Chem. Rev.* **1996**, *96*, 2237−3042. (b) Murahashi, S.-I. *Angew. Chem., Int. Ed. Engl.* **1995**, *34*, 2443. (c) *Organic Peroxides*; Ando, W., Ed.; Wiley: Chichester, U.K., 1992.

(3) (a) Sheldon, R. A.; Kochi, J. K. *Metal-Catalyzed Oxidations of Organic Compounds*; Academic Press: New York, 1981. (b) Patai, S. *The chemistry of peroxides*; John Wiley & Sons: Chichester, U.K., 1983. (c) Martel, A. E.; Sawyer, D. T. *Oxygen Complexes and Oxygen Activation by Transition Metals*; Plenum Press: New York, 1988. (d) Ando, W. *Organic Peroxides*; John Wiley and Sons: Chichester, U.K., 1992. (e) Thematic issue of metal−dioxygen complexes: *Chem. Rev.* **1994**, *94*, 567. (f) Strukul, G. *Angew. Chem., Int. Ed.* **1998**, *37*, 1198. (g) Akita, M.; Moro-oka, Y. *Catal. Today* **1998**, *44*, 183.

10.1021/ic020355e CCC: $22.00
Published on Web 09/13/2002

Scheme 1

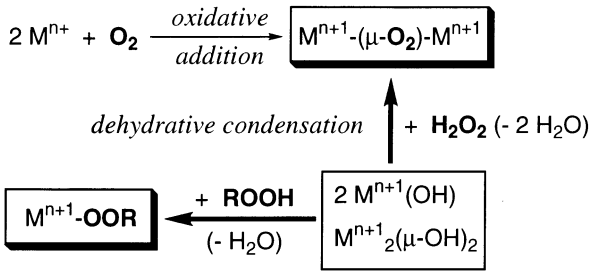

(2) mononuclear alkyl- and hydroperoxo species (M−OOX) could be accessible via condensation with the corresponding hydroperoxide (XOOH). Herein we describe the results of synthesis and characterization of a series of peroxopalladium complexes bearing the (Tp^{iPr2})(py)Pd fragment, (Tp^{iPr2})(py)-Pd−OOX (X = H, R, Pd). This work has been done as a part of the systematic synthetic study of dioxygen complexes supported by hydrotris(pyrazolyl)borato ligand (Tp$^{R'}$),[6−8] and the dehydrative condensation method works most effectively with the present Pd system.[9]

Experimental Section

General Methods. All manipulations were carried out under Ar atmosphere using the standard Schlenk tube technique. THF, ether, benzene, toluene, pentane, hexane (Na−K/benzophenone), and CH_2Cl_2 (P_2O_5) were dried over appropriate drying agents under Ar and distilled before use. ^{1}H NMR spectra were recorded on a Bruker AC200 spectrometer (^{1}H: 200 MHz). $CDCl_3$, benzene-d_6, toluene-d_8, and pyridine-d_5 for NMR measurements containing 0.5% TMS were dried over molecular sieves and distilled under reduced pressure. IR (KBr pellets) and Raman spectra (excitation at 514.5 nm) were recorded on a JASCO FT/IR 5300 spectrometer and a JASCO NRS-2100 spectrometer, respectively. FD-MS spectra were obtained on a JEOL JMS-700 mass spectrometer. Organic products were identified and quantified by a combination of GLC (Shimadzu GC17A equipped with a PHA0201 capillary column and an FID detector) and GCMS analyses (Shimadzu QP5000 connected to GC17A equipped with a PHA0201 capillary column). The hydroxopalladium complexes (Tp^{iPr2})(py)Pd−OH (**1**) and (Tp^{iPr2}Pd)$_2$(μ-OH)$_2$ (**7**) were prepared according to the procedures reported by us.[10] Other chemicals were used as received without further purification.

Preparation of (Tp^{iPr2})(py)Pd−OOH (2a). To **1** (1.37 g, 2.04 mmol) dissolved in THF (40 mL) was added $MgSO_4$ (ca. 0.5 g) and an 35% aqueous solution of H_2O_2 (300 μL, 3.62 mmol). The resultant mixture was stirred for 70 min at ambient temperature. The color of the mixture changed from pale yellow to deep orange. Filtration through a Celite plug, evaporation of the filtrate under reduced pressure, and crystallization of the resultant residue from ether−hexane gave **2a** as a yellow solid (750 mg, 1.10 mmol, 54% yield). ^{1}H NMR (C_6D_6): δ_H 8.60 (2H, m, *o*-py), 6.70 (1H, m, *p*-py), 6.37 (2H, m, *m*-py), 1.64−1.04, 0.70 (m, 36H, CH*Me*$_2$); for other signals, see Table 2. Anal. Calcd for $C_{32}H_{52}N_7BO_2Pd$: C, 56.18; H, 7.68; N, 14.34. Found: C, 56.08; H, 7.51; N, 14.17.

Preparation of (Tp^{iPr2})(Ph$_3$P)Pd−OOH (2b). An ethereal solution (6 mL) of a mixture of **2a** (166 mg, 0.243 mmol) and PPh_3 (63.5 mg, 0.242 mmol) was stirred for 2 h at ambient temperature. After removal of the volatiles under reduced pressure the resultant residue was crystallized from CH_2Cl_2−hexane to give **2b** as deep orange crystals (73.1 mg, 0.177 mmol, 73% yield). ^{1}H NMR ($CDCl_3$): δ_H 7.99 (2H, br, Ph), 7.56−7.07 (11H, m, Ph), 6.65 (2H, m, Ph), 1.65−1.14 (m, 24H, CH*Me*$_2$), 0.78, 0.71, 0.69, 0.05 (3H × 4, d × 4, J = 6.8 Hz, CH*Me*$_2$). ^{31}P NMR ($CDCl_3$): δ_P 20.1. Anal. Calcd for $C_{45}H_{62}N_6BO_2PPd$: C, 62.31; H, 7.22; N, 9.69. Found: C, 62.46; H, 7.40; N, 10.01.

Preparation of (Tp^{iPr2})(py)Pd−OOBu^t (3). To a benzene solution (15 mL) of **1** (619 mg, 0.927 mmol) was added ^{t}BuOOH (70% ^{t}BuOO−^{t}Bu solution, 0. 7 mL, 5.1 mmol), and the resultant mixture was stirred overnight at ambient temperature. Removal of the volatiles under reduced pressure followed by crystallization from acetonitrile at −20 °C gave **3** as yellow crystals (343 mg, 0.464 mmol, 50% yield). ^{1}H NMR (C_6D_6): δ_H 9.31 (2H, m, *o*-py), 6.74 (1H, m, *p*-py), 6.49 (2H, m, *m*-py), 1.66−1.21 (m, 30H, CH*Me*$_2$), 0.98, 0.66 (3H × 2, d × 2, J = 6.8 Hz, CH*Me*$_2$). Anal. Calcd for $C_{36}H_{60}N_3BO_2Pd$: C, 58.41; H, 8.19; N, 13.25. Found: C, 58.48; H, 8.11; N, 13.41.

Preparation of [(Tp^{iPr2})(py)Pd]$_2$(μ-O$_2$) (4). A toluene solution (20 mL) of an equimolar mixture of **1** (219 mg, 0.328 mmol) and **2a** (226 mg, 0.329 mmol) was stirred for 6 h at ambient temperature in the presence of $MgSO_4$ (ca. 0.5 g). After filtration through a Celite plug, pyridine (0.1 mL) was added to the filtrate. Then the volatiles were removed under reduced pressure and the resultant residue was extracted with ether and filtered through a Celite plug. Addition of pentane and cooling at −20 °C gave **4** as dark red orange crystals (240 mg, 0.180 mmol, 55% yield). ^{1}H NMR

(4) (a) Kitajima, N.; Fujisawa, K.; Moro-oka, Y. *J. Am. Chem. Soc.* **1989**, *111*, 8975. (b) Kitajima, N.; Fujisawa, K.; Fujimoto, C.; Moro-oka, Y.; Hashimoto, S.; Kitagawa, T.; Toriumi, K.; Tatsumi, K.; Nakamura, A. *J. Am. Chem. Soc.* **1992**, *114*, 1277. (c) Kitajima, N.; Moro-oka, Y. *Chem. Rev.* **1994**, *94*, 737.

(5) (a) Kitajima, N.; Hikichi, S.; Tanaka, M.; Moro-oka, Y. *J. Am. Chem. Soc.* **1993**, *115*, 5496. (b) Akita, M.; Takahashi, Y.; Hikichi, S.; Moro-oka, Y. *Inorg. Chem.* **2001**, *40*, 169. (c) Kujime, M.; Hikichi. S.; Akita. M. *Organometallics* **2001**, *20*, 4049. (d) See also references cited in refs 6 and 23.

(6) (a) Review: Akita, M.; Hikichi, S. *Bull. Chem. Soc. Jpn.* **2002**, *75*, 1657. Co, Ni: (b) Hikichi, S.; Komatsuzaki, H.; Kitajima, N.; Akita, M.; Mukai, M.; Kitagawa, T.; Moro-oka, Y. *Inorg. Chem.* **1997**, *36*, 266. (c) Hikichi, S.; Komatsuzaki, H.; Akita, M.; Moro-oka, Y. *J. Am. Chem. Soc.* **1998**, *120*, 4699. (d) Hikichi, S.; Yoshizawa, M.; Sasakura, Y.; Akita, M.; Moro-oka, Y. *J. Am. Chem. Soc.* **1998**, *120*, 10567. (e) Hikichi, S.; Yoshizawa, M.; Sasakura, Y.; Komatsuzaki, H.; Akita, M.; Moro-oka, Y. *Chem. Lett.* **1999**, 979. (f) Hikichi, S.; Yoshizawa, M.; Sasakura, Y.; Komatsuzaki, H.; Akita, M.; Moro-oka, Y. *Chem.—Eur. J.* **2001**, *7*, 5011. Fe: (g) Hikichi, S.; Ogihara, T.; Fujisawa, K.; Kitajima, N,; Akita, M.; Moro-oka, Y. *Inorg. Chem.* **1997**, *36*, 4539. (h) Ogihara, T.; Hikichi, S.; Kitajima, N,; Akita, M.; Moro-oka, Y. *Inorg. Chem.* **1998**, *37*, 2614. (i) Ogihara, T.; Hikichi, S.; Kitajima, N,; Akita, M.; Uchida, T.; Kitagawa, T.; Moro-oka, Y. *Inorg. Chim. Acta* **2000**, *297*, 162. Mn: (j) Komatsuzaki, H.; Nagasu, Y.; Suzuki, K.; Shibasaki, T.; Satoh, S.; Ebina, F.; Hikichi, S.; Akita, M.; Moro-oka, Y. *J. Chem. Soc., Dalton Trans.* **1998**, 511. (k) Komatsuzaki, H.; Hikichi, S.; Akita, M.; Moro-oka, Y. *Inorg. Chem.* **1998**, *37*, 6554. (l) V: Kosugi, M.; Hikichi, S.; Akita, M.; Moro-oka, Y. *J. Chem. Soc., Dalton Trans.* **1999**, 1369. (m) Rh: Takahashi, Y.; Hashimoto, M.; Hikichi, S.; Akita, M.; Moro-oka, Y. *Angew. Chem., Int. Ed.* **1999**, *38*, 3074. (n) Ru: Takahashi, Y.; Hikichi, S.; Akita, M.; Moro-oka, Y. *J. Chem. Soc., Chem. Commun.* **1999**, 1491.

(7) (a) Trofimenko, S. *Scorpionates-The Coordination Chemistry of Polypyrazolylborate Ligands*; Imperial College Press: London, 1999. (b) Torofimenko, S. *Chem. Rev.* **1993**, *93*, 943. (c) Kitajima, N.; Tolman, W. B. *Prog. Inorg. Chem.* **1995**, *43*, 419.

(8) Abbreviations used in this paper: Tp$^{R'}$, hydrotris(pyrazolyl)borato ligands; Tp^{iPr2}, 3,5-diisopropylpyrazolyl derivative; pz, pyrazolyl group in Tp$^{R'}$; 4-pz-H, hydrogen atom at the 4-position of the pyrazolyl ring.

(9) Akita, M.; Miyaji, T.; Hikichi, S.; Moro-oka, Y. *J. Chem. Soc., Chem. Commun.* **1998**, 1005. Akita, M.; Miyaji, T.; Hikichi, S.; Moro-oka, Y. *Chem. Lett.* **1999**, 813.

(10) Akita, M.; Miyaji, T.; Muroga, N.; Mock-Knoblauch, C.; Hikichi, S.; Adam, W.; Moro-oka, Y. *Inorg. Chem.* **2000**, *39*, 2096.

(11) Higashi, T. *Program for absorption correction*; Rigaku Corp.: Tokyo, 1995.

Table 1. Crystallographic Data for Peroxopalladium Complexes

param	**2b**·$2CH_2Cl_2$	**3**	**4**·$2C_5H_{12}$	**5**·Et_2O	**8**·Et_2O·0.5(hexane)
formula	$C_{47}H_{66}BN_6O_2PCl_4Pd$	$C_{36}H_{60}BN_7O_2Pd$	$C_{74}H_{126}B_2N_{14}O_2Pd_2$	$C_{63}H_{107}B_2N_{13}O_3Pd_2$	$C_{68}H_{119}O_4B_2Pd_2$
fw	1037.04	1480.24	1478.35	1329.04	1431.2
cryst system	orthorhombic	triclinic	orthorhombic	triclinic	triclinic
space group	$Pna2_1$	$P\bar{1}$	Pbca	$P\bar{1}$	$P\bar{1}$
a/Å	21.1718(11)	13.002(7)	18.791(3)	14.324(7)	15.062(1)
b/Å	16.9093(7)	14.580(7)	22.280(3)	20.487(8)	22.885(2)
c/Å	14.7058(6)	11.29(1)	19.158(4)	13.161(8)	12.3043(8)
α/deg		109.69(6)		92.24(4)	104.168(1)
β/deg		92.41(7)		104.75(3)	103.024(5)
γ/deg		88.66(5)		106.99(2)	92.205(2)
V/Å^3	5264.7(4)	2014(3)	8021(2)	3545(3)	3986.6(5)
Z	4	2	4	2	2
d_{calcd}/g cm^{-3}	1.308	1.221	1.224	1.245	1.19
μ/mm^{-1}	0.627	0.499	0.499	0.557	0.502
2θ/deg	up to 54.9	up to 54.4	up to 54.4	up to 54.0	up to 55.0
no of params refined	583	439	438	788	818
R1 for data with $I > 2\sigma(I)$	0.0825 (for 5640 data)	0.0819 (for 7578 data)	0.0542 (for 7514 data)	0.0827 (for 9471 data)	0.081 (9721 data)
wR2 (for all 5905 data)	0.2218 (for all 7854 data)	0.2212 (for all 8006 data)	0.1563 (for all 11 614 data)	0.2345 (for all 15 065 data)	0.208

(CD_2Cl_2 at −30 °C): δ_H 1.5−0.5 (36H, Me); py signals could not be located, because the ^{1}H NMR spectrum was recorded in the presence of py-d_5 to suppress the dissociation process (Scheme 3) and the added py-d_5 exchanged with the coordinated py rapidly. Anal. Calcd for $C_{64}H_{102}N_6B_2O_2Pd_2$: C, 57.61; H, 7.72; N, 14.70. Found: C, 57.44; H, 8.01; N, 14.81.

Preparation of (Tp^{iPr2})(py)Pd−μ-κ^1:κ^2-O_2−Pd(Tp^{iPr2}) (5). A CH_2Cl_2−hexane solution (1:3, 20 mL) of **2a** (164 mg, 0.240 mmol) and **7** (141 mg, 0.120 mmol) was stirred for 8 h at room temperature in the presence of $MgSO_4$ (200 mg). Filtration through a Celite plug, concentration of the filtrate under reduced pressure, and cooling at −30 °C gave **5** as orange crystals (119 mg, 0.095 mmol, 40% yield). ^{1}H NMR (pyridine signals; CD_2Cl_2): at room temperature, δ_H 8.57 (1H), 7.36 (2H), 6.89 (2H), 1.3−0.3 (36H, Me); at −80 °C, δ_H 9.03, 7.84, 7.36, 6.88, 6.71 (1H each), 1.4−0.4 (36H, Me). Anal. Calcd for $C_{59}H_{97}N_{13}B_2O_2Pd_2$: C, 56.47; H, 7.79; N, 14.51. Found: C, 56.22; H, 7.76; N, 14.29.

Preparation of 8 from 2a and CH_3CN. An acetonitrile solution (10 mL) of **2a** (69 mg, 0.10 mmol) was stirred for 3 h at ambient temperature. Concentration of the solution to ca. 3 mL followed by cooling at −30 °C gave **8** as orange crystals (52 mg, 0.040 mmol, 80% yield). ^{1}H NMR (C_6D_6): δ_H 9.75 (2H, d, J = 5 Hz, *o*-py), 6.83 (1H, t, J = 7 Hz, *p*-py), 6.68 (2H, m, *m*-py), 6.09, 6.04, 6.03, 6.02, 5.86, 5.79 (1H × 6, s × 6, 4-pz-H), 4.01−2.89 (1H × 12, m, C*H*Me$_2$), 1.87−0.62 (72H, m, CH*Me$_2$*), 1.34 (3H × 1, s, Me). IR: 2476 (ν_{BH}), 1588 cm^{-1} ($\nu_{C=N}$). Anal. Calcd for $C_{61}H_{102}N_{14}B_2O_3Pd_2$ (**8**·H_2O): C, 55.76; H, 7.82; N, 14.92. Found: C, 55.99; H, 7.92; N, 14.81. ^{1}H NMR experiments were carried out in C_6D_6 and quantified using the residual C_6D_5H signal as an internal standard.

Oxygenation of Acetaldehyde. A THF solution (10 mL) of **2a** (193 mg, 0.282 mmol) and acetaldehyde (0.5 mL, 8.9 mmol) was stirred for 5 h at room temperature. Concentration under reduced pressure, addition of hexane, and cooling at −30 °C gave **9** as yellow crystals (110 mg, 0.154 mmol, 55% yield). The acetato complex **9** was identified by comparison of its spectral data with those reported in our previous paper.[11] NMR experiments were done in C_6D_6 and quantified using the residual C_6D_5H signal as an internal standard.

X-ray Crystallography. Crystallographic data and results of structure refinements are summarized in Table 1. Single crystals of **2b** (CH_2Cl_2−hexane), **3** (MeCN), **4** (Et_2O−pentane), **5** (Et_2O−hexane), and **8** (Et_2O−hexane) were obtained by recrystallization from the solvent systems shown in the parentheses and mounted on glass fibers.

Diffraction measurements were made on a Rigaku RAXIS IV imaging plate area detector with Mo Kα radiation (λ = 0.710 69 Å) at −60 °C. The data collections were controlled by the software obtained from the Rigaku Corp., Tokyo, Japan [raxis (**2b**, **3**−**5**), rapid (**8**)]. The crystal-to-detector distance was 110 mm ($2\theta_{max}$ = ∼55°). Indexing was performed from 3 oscillation images which were exposed for 4 min. The detector swing angle, the number of oscillation images, and the exposed time were as follows: **2b**, 3.0°/23/50 min/deg; **3**, 6.0°/30/75 min/deg; **4**, 3.0°/20/40 min/deg; **5**, 6.0°/27/90 min/deg; **8**, 3.0°/60/15 min/deg. Readout was performed with the pixel size of 100 μm × 100 μm. In the reduction of data, Lorentz and polarization corrections and empirical absorption corrections were made.[11]

The structural analysis was performed on an IRIS O2 computer using the teXsan structure-solving program system obtained from the Rigaku Corp., Tokyo, Japan.[12] Neutral scattering factors were obtained from the standard source.[13]

The structures were solved by a combination of the direct methods (SHELXS-86[14] or SIR92[15]) and Fourier synthesis (DIRDIF94).[16] Least-squares refinements were carried out using SHELXL-97[14] (refined on F^2) linked to teXsan. Unless otherwise stated, all the non-hydrogen atoms were refined anisotropically, riding refinements were applied to the methyl hydrogen atoms [B(H) = B(C)], and the other hydrogen atoms were fixed at the calculated positions. During the refinements of **2b** and **5**, a part of the isopropyl groups was found to be disordered and refined by taking into account two components (**2b**, C38:C38A = 0.48:0.52; **5**, C58,59:C58A,59A = 0.46:0.54) and hydrogen atoms attached to the disordered atoms were not included in the refinements. For **8**, the ether and hexane solvates were refined isotropically and two components were taken into account for the ether solvate (O91, C93:O91A,C93A = 0.5:0.5).

(12) *teXsan; Crystal Structure Analysis Package*, *ver. 1. 11*; Rigaku Corp.: Tokyo, 2000.
(13) *International Tables for X-ray Crystallography*; Kynoch Press: Birmingham, U.K., 1975; Vol. 4.
(14) (a) Sheldrick, G. M. *SHELXS-86: Program for crystal structure determination*; University of Göttingen: Göttingen, Germany, 1986. (b) Sheldrick, G. M. *SHELXL-97: Program for crystal structure refinement*; University of Göttingen: Göttingen, Germany, 1997.
(15) Altomare, A.; Burla, M. C.; Camalli, M.; Cascarano, M.; Giacovazzo, C.; Guagliardi, A.; Polidori, G. *J. Appl. Crystallogr.* **1994**, *27*, 435.
(16) Beurskens, P. T.; Admiraal, G.; Beurskens, G.; Bosman, W. P.; Garcia-Granda, S.; Gould, R. O.; Smits, J. M. M.; Smykalla, C. *The DIRDIF program system, Technical Report of the Crystallography Laboratory*; University of Nijmegen: Nijmegen, The Netherland, 1992.

Scheme 2

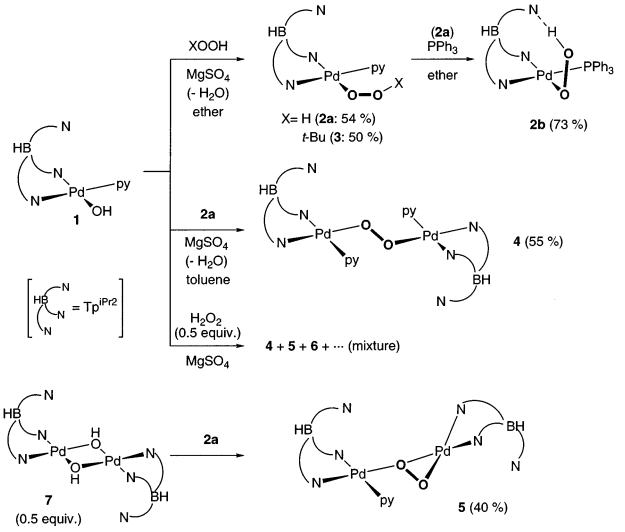

Results and Discussion

Synthesis of a Series of Peroxopalladium Complexes via Dehydrative Condensation of Hydroxopalladium Complex (κ^2-Tp^{iPr2})(py)Pd−OH (1) with ROOH. In a previous paper[10] we reported the synthesis and characterization of the square-planar hydroxopalladium complex (κ^2-Tp^{iPr2})(py)Pd−OH (**1**), and it was also found that complex **1** readily underwent dehydrative condensation with an acidic substrate (H−A) such as phenol and acetic acid to give the corresponding condensates (κ^2-Tp^{iPr2})(py)Pd−A. Reaction of **1** with hydroperoxides (XOOH; X = H, ^{t}Bu) proceeded in a similar manner in the presence of a dehyrating agent such as $MgSO_4$ and Na_2SO_4 to give the (hydroperoxo)- (**2a**) and (*tert*-butylperoxo)palladium complexes (**3**) (Scheme 2),[9] although hydroperoxides are much less acidic than the organic substrates mentioned above (pK_a for *t*-BuOOH: 16.73).[17] While the *tert*-butylperoxo derivative **3** could be characterized crystallographically, a single crystal of **2a** suitable for X-ray crystallography could not be obtained despite many attempts, and then **2a** was converted to the PPh_3 derivative **2b** by treatment with PPh_3 (see below).

Because the resultant (hydroperoxo)palladium complex **2a** was regarded as a hydroperoxide, further condensation of **2a** with **1** would produce the (μ-κ^1:κ^1-peroxo)dipalladium complex **4**, which was actually obtained as red-orange crystals in a moderate yield, as was expected (Scheme 2). For isolation of **4** it was essential to add pyridine at the stage of workup. Otherwise, a mixture containing the expected product **4** and the unsymmetrical monopyridine complex **5** was obtained (see below).

In principle, condensation of **1** with 0.5 equiv of H_2O_2 would afford the (μ-peroxo)dipalladium complex **4** via double dehydrative condensation. Such a reaction, however, resulted in the formation of a complicated mixture containing **4** and other peroxo species, from which two products were isolated and characterized by X-ray crystallography. One of the two products was the orange (μ-κ^1:κ^2-peroxo)dipalladium complex **5**, formation of which was formally explained in terms of elimination of one of the two pyridine ligands in **4**

Chart 1

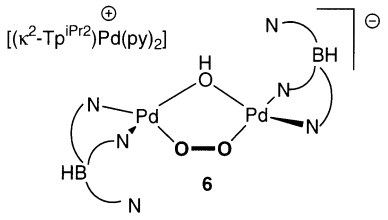

followed by κ^2-coordination of the bridging peroxo ligand to the palladium center that loses the pyridine ligand. Complex **5** was alternatively obtained in a selective manner via dehydrative condensation between bis(μ-hydroxo)dipalladium complex without the pyridine ligand, (Tp^{iPr2}Pd)$_2$(μ-OH)$_2$ (**7**),[10] and **2a** (Scheme 2). The other orange product obtained from **1** and H_2O_2 was an ionic species, [(κ^2-Tp^{iPr2})Pd(py)$_2$]$^+$[(κ^2-Tp^{iPr2})Pd(μ-κ^1:κ^1-OO)(μ-OH)Pd(κ^2-Tp^{iPr2})]$^-$ (**6**), shown in Chart 1. Because an analytically pure sample of complex **6** could not be obtained despite many attempts, the results of X-ray crystallography are included in the Supporting Information.[18] The anionic part of **6** consists of a five-membered cyclic (μ-κ^1:κ^1-peroxo)(μ-hydroxo)dipalladium linkage, and the cationic part is the bis(pyridine) adduct, [(κ^2-Tp^{iPr2})Pd(py)$_2$]$^+$, arising from redistribution of the pyridine ligand in the (Tp^{iPr2})(py)Pd fragment. Many examples containing a 1,3-dimetalla-2,4,5-trioxacyclic structure, M(μ-κ^1:κ^1-OO)(μ-OX)M (X = H or none), have been reported so far, and an analogous cationic diplatinum complex, [(Ph$_3$P)$_2$Pt(μ-κ^1:κ^1-OO)(μ-OH)Pt(PPh$_3$)$_2$]$^+$ClO$_4^-$,[19g] was reported by Hursthouse et al.

Dinuclear μ-κ^2:κ^2-peroxo species, (μ-κ^2:κ^2-O$_2$)M$_2$, have also been recognized as key intermediates of oxygenation reactions as typically shown by the copper complex mimick-

(17) Yuan, L.-C.; Bruice, T. C. *J. Am. Chem. Soc.* **1986**, *108*, 1643.

(18) Crystallographic data for **6**: formula $C_{106}H_{185}B_3N_{20}O_3Pd_3$, [**6**·3(pentane)], fw = 2139.37, space group triclinic *P*1, *a* = 18.351(5) Å, *b* = 22.373(9) Å, *c* = 16.823(5) Å, α = 103.81(3)°, *β* = 109.43(2)°, *γ* = 65.97(2)°, *V* = 5906(3) Å^3, *Z* = 2, d_{calcd} = 1.203 g cm^{-3}, μ = 0.505 mm^{-1}, $2\theta_{max}$ = up to 54.0°, no. of parameters refined = 1177, R1 = 0.1101 (for 13 104 data with $I > 2\sigma(I)$), wR2 = 0.2924 (for all 17 408 data). Selected bond lengths (in Å) and bond angles (in deg) for the anionic part: O1−O2, 1.47(1); Pd1−O1, 1.958(9); Pd1−O3, 2.049(7); Pd1−N11, 2.019(8); Pd1−N21, 2.07(1); Pd2−O2, 1.954(8); Pd2−O3, 2.032(8); Pd2−N41, 2.00(1); Pd2−N51, 2.060(9); Pd1−N31, 4.819(8); Pd2−N61, 3.019(9); Pd1−O1−O2, 106.5(7); Pd2−O2−O1, 108.7(5); Pd1−O3−Pd2, 113.6(4); O1−Pd1−O3, 85.5(3); O2−Pd2−O3, 87.03; Pd1−O1−O2−Pd2, 70.6(5).

(19) Pt−OO(R) complexes: (a) Ugo, R.; Conti, F.; Cenini, S.; Mason, R.; Robertson, G. B. *J. Chem. Soc., Chem. Commun.* **1968**, 1498. (b) Cook, C. D.; Cheng, P.-T.; Nyburg, S. C. *J. Am. Chem. Soc.* **1969**, *91*, 2123. (c) Kashiwagi, T.; Yasuoka, N.; Kasai, N.; Kakudo, M.; Takahashi, S.; Hagihara, N. *J. Chem. Soc. D* **1969**, 743. (d) Cook, C. D.; Cheng, P.-T.; Nyburg, S. C.; Wan, K. Y. *Can. J. Chem.* **1971**, *49*, 3772. (e) Bhaduri, S.; Casella, L.; Ugo, R.; Raithby, P. R.; Zuccaro, C.; Hursthouse, M. B. *J. Chem. Soc., Dalton Trans.* **1979**, 1624. (f) Ferguson, G.; Parvez, M.; Monaghan, P. K.; Puddephatt, R. J. *J. Chem. Soc., Chem. Commun.* **1983**, 267. (g) Read, G.; Urgelles, M.; Galas, A. M. R.; Hursthouse, M. B. *J. Chem. Soc., Dalton Trans.* **1983**, 911. (h) Strukul, G.; Michelin, R. A.; Orbell, J. D.; Randaccio, L. *Inorg. Chem.* **1983**, *22*, 3706. (i) Ferguson, G.; Parvez, M.; Monaghan, P. K.; Puddephatt, R. J. *Organometallics* **1985**, *4*, 1669. (j) Pandolfo, L.; Paiaro, G.; Valle, G.; Ganis, P. *Gazz. Chim. Ital.* **1985**, *115*, 59. (k) Pizzotti, M.; Cenini, S.; Ugo, R.; Demartin, F. *J. Chem. Soc., Dalton Trans.* **1991**, 65. (l) Dieck, H. T.; Fendesak, G.; Munz, C. *Polyhedron* **1991**, *10*, 255. (m) Davies, M. S.; Hambley, T. W. *Inorg. Chem.* **1998**, *37*, 5408. (n) Litz, K. E.; Banaszak Holl, M. M.; Kampf, J. W.; Carpenter, G. B. *Inorg. Chem.* **1998**, *37*, 6461. (o) Wick, D. D.; Goldberg, K. I. *J. Am. Chem. Soc.* **1999**, *121*, 11900.

Table 2. Selected IR and ^{1}H NMR Data for Peroxopalladium Complexes

	IR/cm^{-1} [a]			^{1}H NMR/δ_H [b]		
complex	ν_{BH}	$\nu_{CN(py)}$ [c]	$\nu_{CN(pz)}$ [c]	4-pz-H [d,8]	C*H*Me$_2$ [e]	OOX [d]
2a	2486	1606	1535	6.16, 5.98, 5.87	4.23, 3.69, 3.63, 3.17, 3.09, 2.30	6.86 (OOH)
2b	2483		1535	5.89, 5.64, 5.48	4.09, 3.62, 3.27, 3.19, 2.04, 1.84	8.93 (OOH)
3	2475	1608	1535	6.25, 5.99, 5.86	4.42, 3.80, 3.57, 3.31, 3.13, 2.27	1.01 (OO^{t}Bu) [f]
4	2479	1607	1535	5.65,[g] 5.8−6.1,[h,I] 6.05, 5.93, 5.68, 5.66, 5.62, 5.50[k]	4.6 (br), 2.0−3.7,[j] 4.6, 1.93.6[j]	
5	2476	1605	1535	6.02, 5.89, 5.64,[I] 6.10, 6.00, 5.89, 5.84, 5.60, 5.43[l]	3.77,[g] 3.51,[g] 3.46,[g] 2.77,[h] 2.00,[g] 3.7−1.45[j]	

[a] Observed as KBr pellets. [b] Observed at 200 MHz at rt unless otherwise stated. Solvents: C_6D_6 (**2a**, **3**), $CDCl_3$ (**2b**), CD_2Cl_2 (**4**, **5**). Intensity of the signals is for 1H unless otherwise stated. The other signals are summarized in the Experimental Section. [c] ν_{py} and ν_{pz} refer to the C=C vibration of the pyridine and pyrazolyl rings, respectively. [d] Singlet signals. [e] Septet signals (J = ~7 Hz). [f] Intensity: 9H. [g] Intensity: 2H. [h] Intensity: 4H. [i] Observed at rt. [j] Signals were not resolved due to overlap and/or broadening. [k] Observed at −30 °C. [l] Observed at −80 °C.

ing the active sites of some copper proteins $(Tp^{iPr2}Cu)_2(\mu$-κ^2:κ^2-$O_2)$, which was also prepared by condensation between the bis(μ-hydroxo)dicopper complex analogous to **7**, $(Tp^{iPr2}Cu)_2(\mu$-$OH)_2$, and H_2O_2.[4] To synthesize the dipalladium analogue $(Tp^{iPr2}Pd)_2(\mu$-κ^2:κ^2-$O_2)$ (**A**), **7**[10] was treated with H_2O_2. But no apparent condensation was observed, and complex **7** was recovered unaffected from the reaction mixture. We also attempted synthesis of **A** via, for example, removal of the pyridine ligand(s) in **4** and **5**, but we have not met with success so far (see below).

Characterization of Peroxopalladium Complexes 2−5. (i) Spectroscopic Characterization. The isolable peroxopalladium complexes **2**−**5** are characterized by spectroscopic methods (Table 2). First of all, the Tp^{iPr2} ligand in **2**−**5** is coordinated to the metal center in κ^2-fashion as revealed by the ν_{BH} vibrations observed in the range below 2500 cm^{-1},[20] suggesting square-planar coordination geometry, which is typical for four-coordinate Pd(II) d^8 species and verified by X-ray crystallography (see below).

The O−O stretching vibration is examined for **2**−**5** by means of IR and Raman spectroscopy. For the μ-peroxo complex **4**, a very intense Raman absorption is observed at 838 cm^{-1} in addition to weak signals at 1026 and 886 cm^{-1} (less than 1/5 in height). Because the weak signals appear in essentially the same positions as the signals observed for the hydroxo complex **1** (1026, 888 cm^{-1}), which does not possess the O−O linkage but the (Tp^{iPr2})(py)Pd−O structural motif, the absorption at 838 cm^{-1} has been assigned to O−O stretching vibration. The ν_{O-O} value of **4** is comparable to that of the analogous (μ-κ^1:κ^1-peroxo)dicopper complex, $((TMPA)Cu)_2(\mu$-$O_2)$ [ν_{O-O} = 832 cm^{-1}; TMPA = tris(pyridylmethylamine)].[21] For the other complexes, although a weak Raman band is observed for the *tert*-butylperoxo complex **3** in the same range (848 cm^{-1}), any notable difference in IR and Raman spectra has not been detected for **2a** and **5** when compared with the hydroxo complex **1**. Thus, the O−O vibration has been located only for the highly symmetrical complex **4** by Raman spectroscopy.

The *tert*-butylperoxo complex **3** is unequivocally characterized by spectroscopic methods. In addition to the above-mentioned κ^2-coordinated Tp^{iPr2} ligand, coordination of a pyridine and a *tert*-butylperoxo ligand is confirmed by ^{1}H NMR completing the square-planar Pd(II) coordination environment. In accord with the unsymmetrical structure the three 4-pz-H signals [8] are observed separately.

Chart 2

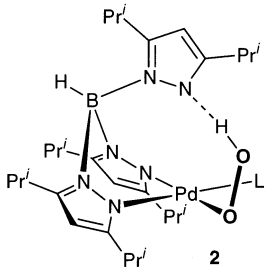

2

The two hydroperoxo complexes **2a,b** show spectroscopic features similar to those of the *tert*-butylperoxo derivative **3**: (1) ν_{BH} < 2500 cm^{-1};[20] (2) the presence of a pyridine or PPh_3 ligand (^{1}H NMR and IR); (3) the three inequivalent 4-pz-H signals [8] (^{1}H NMR) (Table 2). The OOH signals of **2a,b** (^{1}H NMR), which disappears upon addition of D_2O, are located in considerably low field [δ_H 6.86 (**2a**), 8.93 (**2b**)] when compared with the OH signal of the starting hydroxo complex **1** (δ_H −1.79) suggesting a structural change, but the ν_{OH} vibration of the OOH group cannot be located in both cases. This could be ascribed to the hydrogen-bonding interaction between the OOH group with the nitrogen atom of the pendant noncoordinated pyrazolyl group of the Tp^{iPr2} ligand (Chart 2) as revealed for the PPh_3 derivative **2b** with the aid of X-ray crystallography (see below).

The pyridine ligand was found to be labile, because addition of pyridine-d_5 to a benzene-d_6 solution of **2**−**5** resulted in displacement of the coordinated pyridine ligand by pyridine-d_5. In addition to this ligand exchange process, the dinuclear complexes **4** and **5** exhibit dynamic behavior in solutions. A ^{1}H NMR spectrum of the μ-κ^1:κ^1-peroxo complex **4** dissolved in C_6D_6 shows formation of a ca. 1:1 mixture of **4** and **5** with liberation of a pyridine molecule (Scheme 3 i). On the other hand, addition of pyridine to **5** gives **4** (Scheme 3ii). In addition, the unsymmetrical complex **5** provides a ^{1}H NMR spectrum with a single set of the Tp^{iPr2} signals at room temperature featuring a symmetrical structure. This spectral feature suggests occurrence of dynamic behavior, and upon lowering of the temperature to −80 °C the three 4-pz-H signals separate into six signals resulting from two inequivalent Tp^{iPr2} groups as is consistent with the solid-state structure. The dynamic behavior can be interpreted in terms of dissociation equilibrium of the pyridine ligand,

(20) Akita, M.; Ohta, K.; Takahashi, Y.; Hikichi, S.; Moro-oka, Y. *Organometallics* **1997**, *16*, 4121.
(21) Tyeklár, S.; Jacobsen, R. R.; Wei, N.; Murthy, N. N.; Zubieta, J.; Karlin, K. D. *J. Am. Chem. Soc.* **1993**, *115*, 2677.

Scheme 3

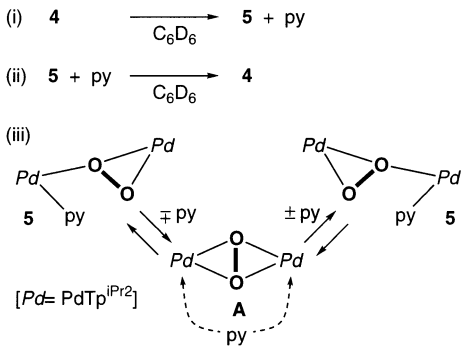

which proceeds by way of the μ-κ^2:κ^2-peroxo intermediate **A** (Scheme 3iii), although **A** has never been detected so far. The broad 4-pz-H signals[8] for **4** results from dynamic behavior via a trigonal-bipyramidal intermediate, which averages the two pyrazolyl rings of the Tp^{iPr2} ligand in the basal plane. Similar behavior has been noted for the related square-planar (Tp$^{R'}$)(L)Pd−X-type complexes.[22]

(ii) Crystallographic Characterization. Molecular structures of the **(**hydroperoxo)- (**2b**), (*tert*-butylperoxo)- (**3**), and (μ-peroxo)palladium complexes (**4**, **5**) have been determined by X-ray crystallography. Their molecular structures are shown in Figures 1 and 2, and selected structural parameters are compared in Table 3.

Only two examples of structurally characterized peroxopalladium complexes, the cyclic peroxo complex (PhBu$^t_2$P)$_2$Pd(κ^2-O$_2$) [23a] and the tetrameric *tert*-butylperoxo complex (μ-κ^1:κ^1-Cl$_3$CCOO)$_4$Pd$_4$(μ-κ^1-OOBu^t)$_4$,[23b] are found in the CSDS database in addition to the Tp^{iPr2}Pd complexes reported by us,[9] although much more examples of platinum complexes, lower congeners, are known.[19]

The (Tp^{iPr2})(py)Pd moieties in the (Tp^{iPr2})(py)Pd−OOX-type complexes **2**−**4** and **5** (Pd1 part) adopt the square-planar geometry with the κ^2-Tp^{iPr2} ligand as is suggested by the IR data (ν_{BH}).[20] The lack of bonding interaction between the palladium center and the nitrogen atom of the pendant pyrazolyl ring is evident from the interatomic distances between them [3.07(1)−3.603(8) Å], which are substantially longer than the Pd−N distances in the basal plane (∼2.0 Å) and exceed the range of bonding interaction. The structural features of the (κ^2-Tp^{iPr2})(py)Pd moieties except for **2b** (see below) are very similar to those in the (κ^2-Tp$^{R'}$)(py)Pd−X-type square-planar complexes (X = Cl, OH, enolato) reported in our previous papers.[5c,10] The Pd2 part of **5** adopts a distorted square-planar geometry, in which the two *cis*-basal coordination sites are occupied by the bridging peroxo ligand with the O−O separation of 1.439(8) Å. The N51−N61−Pd2−O1−O2 moiety is essentially planar as is indicated by (1) the small deviation of the O1 (0.17 Å) and O2 atoms (0.14 Å) from the Pd2−N51−N61 plane and (2) the dihedral angle between the Pd2−N51−N61 and Pd2−O1−O2 planes (4.7°).

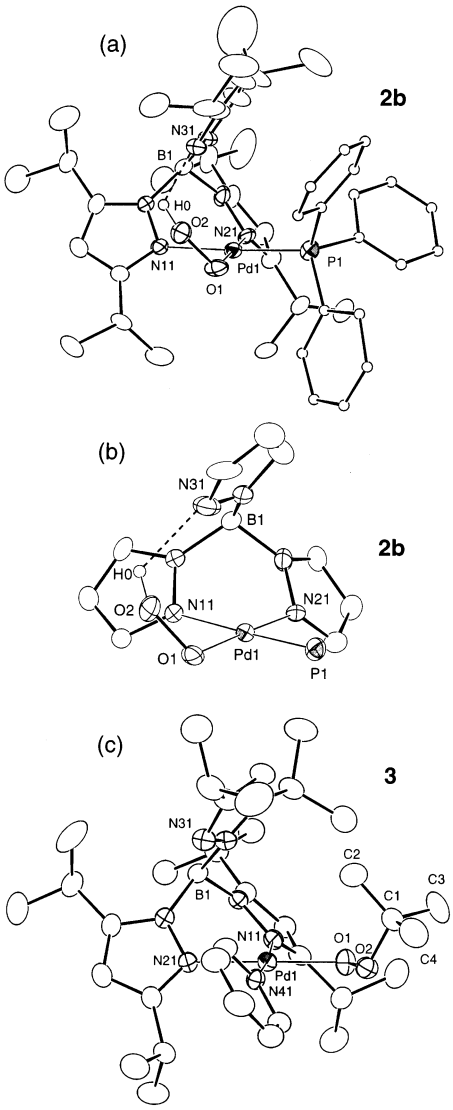

Figure 1. Molecular structures of **2b** and **3** drawn with thermal ellipsoids at the 30% probability level: (a) overview of **2b**; (b) expanded view of the core part of **2b**; (c) an overview of **3**.

As for the peroxo moieties, the O−O and Pd−O lengths and the Pd−O−O angles are very similar with each other. The O−O lengths [1.436−1.463(9) Å], which are in the range of O−O single bonds, are typical for peroxo ligands (O_2^{2-}) and comparable to those for previously reported dinuclear μ-κ^1:κ^1-peroxo and mononuclear cyclic κ^2-peroxo complexes.[3] The Pd−O−O angles of ca. 110° (except Pd2−O2−O1 in **5**) are also typical for M−O−O−X-type peroxometal complexes indicating sp^3-hybridization of the O−O atoms as is consistent with the assignment as a peroxide (O_2^{2-}). Although the κ^2-O$_2$ coordination to the Pd2 center in **5** results in distortion of the Pd2 square-planar coordination geometry as mentioned above, such a coordination mode does not cause a significant change in the O−O length. The dihedral angle between the planes defined by the O1−O2−Pd1 and O1−O2−Pd2 atoms is 127.1° indicating a folded conformation of the Pd(μ-κ^1:κ^2-O$_2$)Pd core as well as the sp^3-hybridization of the O$_2$ oxygen atoms.

It should be noted that the Pd1···N31 distance in the hydroperoxo complex **2b** [3.07(1) Å] is considerably shorter

(22) Goto, N.: Tanaka, M.; Kujime, M.; Hikichi, S.; Akita, M. To be published.
(23) (a) Yoshida, T.; Tatsumi, K.; Matsumoto, M.; Nakatsu, K.; Nakamura, A.; Fueno, T.; Otsuka, S. *New J. Chem.* **1979**, *3*, 761. (b) Mimoun, H.; Charpentier, R.; Mitschler, A.; Fischer, J.; Weiss, R. *J. Am. Chem. Soc.* **1980**, *102*, 1047.

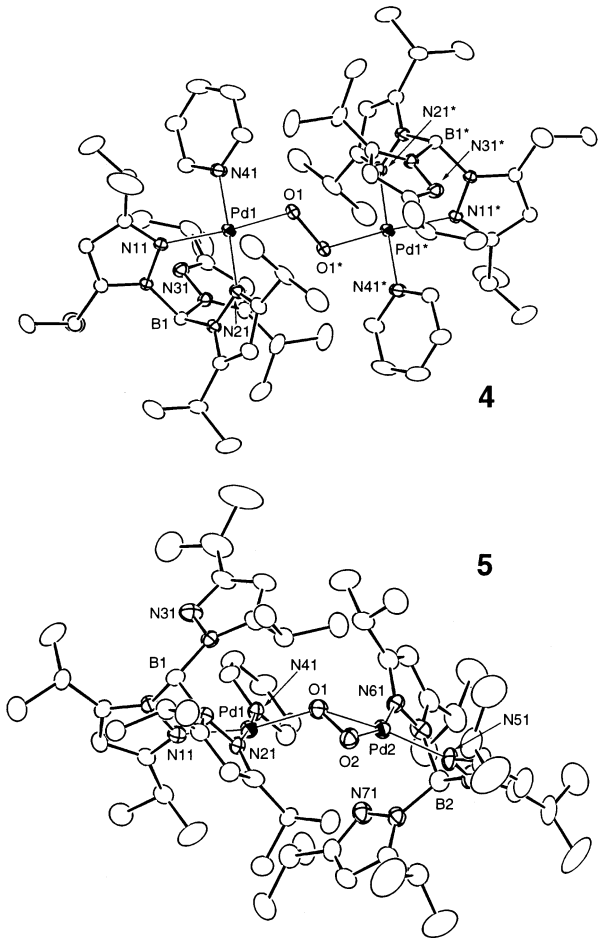

Figure 2. Molecular structures of **4** and **5** drawn with thermal ellipsoids at the 30% probability level.

than those for the other complexes (by ~0.5 Å) suggesting an additional interaction at the pendant pz group. When the orientation of the pendant pyrazolyl rings is closed up (Figure 1b), the lone pair electrons of the N31 atoms of the other complexes (and N71 atom in **5**) are projected away from the Pd center but those in **2b** are directed toward the square-planar coordination plane. These distinct features can be ascribed to hydrogen-bonding interaction between the lone pair electrons of N31 and the hydrogen atom (H1) of the hydroperoxo ligand (Chart 2). Such an interaction is consistent with the O2···N31 separation [2.88(1) Å] and the fact that ν_{OH} vibration cannot be located in the IR spectrum (see above). On the basis of the similar spectroscopic features of **2a,b**, the pyridine-coordinated derivative **2a** is concluded to involve an analogous hydrogen-bonding interaction.

Hydroperoxo species has been regarded as a key intermediate of a variety of oxygenation reactions,[24] but to the best of our knowledge, only eight examples of structurally characterized transition metal hydroperoxo complexes (including **2b**) have been reported so far: $\{[(en)_2Co]_2(\mu\text{-}OOH)(\mu\text{-}NH_2)\}^{4+}$ (**B**);[25a] $\{[(O_2)_2(O)Mo]_2(\mu\text{-}OOH)_2\}^{2-}$ (**C**);[25b] Cp*Ir(μ-κ^1:κ^1-pz)$_3$Rh(dppe)−OOH (**D**) (pz: pyrazolyl);[25c] [(dppa)-Cu−OOH]$^+$ (**E**);[25d] (Tp^{iPr2})(pz)(pz-H)Rh−OOH (**F**);[6m] [(Tp^{Me2})Me$_2$Pt−OOH]$_2$ (**G**);[25e] [(L)(MeCN)Co−OOH]ClO$_4$ (**H**) (L = *meso*-5,7,7,12,14,14-Me$_6$-[14]aneN$_4$).[25f] This is presumably owing to the extreme thermal instability of such a type of compound, but most of the structurally characterized complexes are found to be thermally stable. It is notable that (1) three of the eight examples are supported by a Tp$^{R'}$ ligand (**2b**, **F**, and **G**) and (2) hydrogen-bonding interaction of the OOH group is found for five examples (**2b**, **E**−**H**). Previously reported hydrogen-bonding interaction modes are shown in Chart 3. Both of the α- and β-oxygen atoms can take part in the hydrogen-bonding interaction with a donor part close to them, usually an N-donor. Complex **2** belongs to the **I**-type structure, which has been found in the related (hydroperoxo)rhodium complex **F** reported by us. Typical examples of the **J**- and **K**-type structures are **E** and **G**, respectively. But hydrogen-bonding interaction is not essential, because complexes without such stabilization (e.g. **D**) are known.

(μ-κ^1:κ^1-Peroxo)dimetal complexes (like **4**) and unsymmetrical (μ-κ^1:κ^2-peroxo)dimetal complexes (like **5**) have many precedents, in particular, for Co complexes[26a,b] and V, Mo, and W complexes, respectively. Typical examples and their O−O distances are as follows. μ-κ^1:κ^1-(OO)(ML)$_2$: ML = Co(bipy)(terpy) [1.419(7) Å],[26c] Co(tacn^{Me3})(acac) [1.413-(6) Å],[26d] Co(phen)(bpa) [1.436 Å; bpa = bis(2-pyridylmethyl)-amine],[26e] Cu(tpa) [1.432(6) Å; tpa = tris(2-pyridylmethyl)-amine];[26f] (O$^-$)(O$_2$)$_2$V(μ-κ^1:κ^2-OO)V(O$_2$)$_2$(OH$_2$)(O$^-$) [1.477(6) Å],[27a] (μ-κ^1:κ^2-OO)$_2$[RhCl(PPh$_3$)$_2$]$_2$ [1.44(1) Å].[27b] The structural features of **4** and **5** including the O−O distances [1.447-(4) (**4**) and 1.439(8) Å (**5**)] are very similar to those of these precedents.

Stability and Reactivity of Peroxopalladium Complexes. The peroxopalladium complexes **2**−**4** are found to be quite stable compared to derivatives of other transition metal complexes, in particular, first row metal complexes. This is partly due to the redox-inactive nature of the palladium center in these complexes. When a benzene-d_6 solution of the *tert*-butylperoxo complex **3** was heated to 85 °C, it took 3 h for its complete decomposition. The other complexes **2a**, **4**, and **5** gradually decomposed over the course of 1−3 days when left at room temperature. As for

(24) See, for example: Chen, K.; Costas, M.; Kim, J.; Tipton, A. K.; Que, Jr., L. *J. Am. Chem. Soc.* **2002**, *124*, 3026. Wada, A.; Ogo, S.; Nagatomo, S.; Kitagawa, T.; Watanabe, Y.; Jitsukawa, K.; Masuda, H. *Inorg. Chem.* **2002**, *41*, 616. See also references therein.

(25) (a) Thewalt, U.; Marsh, R. *J. Am. Chem. Soc.* **1967**, *89*, 6364. (b) Le Carpentier, J.-M.; Mitschler, A.; Weiss, R. *Acta Crystallogr., Sect. B* **1972**, *28*, 1288. (c) Carmona, D.; Lamata, M. P.; Ferrer, J.; Modrego, J.; Perales, M.; Lahoz, F. J.; Atencio, R.; Oro, L. A. *J. Chem. Soc., Chem. Commun.* **1994**, 575. (d) Wada, A.; Harata, M.; Hasegawa, K.; Jitsukawa, K.; Masuda, H.; Mukai, M.; Kitagawa, T.; Einaga, H. *Angew. Chem., Int. Ed. Engl.* **1998**, *37*, 798. (e) Wick, D. D.; Goldberg, K. I. *J. Am. Chem. Soc.* **1999**, *121*, 11900. (f) Guzei, I. A.; Bakac, A. *Inorg. Chem.* **2001**, *40*, 2390.

(26) (a) Niederhoffer, E. C.; Timmons, J. H.; Martel, A. E. *Chem. Rev.* **1984**, *84*, 137. (b) Buckingham, D. A.; Clark, C. R., In *Comprehensive Coordination Chemistry*; Wilkinson, G., Ed.; Pergamon: Oxford, U.K., 1987; Vol. 4, Chapter 47, pp 775−789. (c) Ramprasad, D.; Gilicinski, A. G.; Markley, T. J.; Pez, G. P. *Inorg. Chem.* **1994**, *33*, 2841. (d) Hayashi, Y.; Obata, M.; Suzuki, M.; Uehara; A. *Chem. Lett.* **1997**, 1255. (e) Hartshom, R. M.; Telfer, S. G. *J. Chem. Soc., Dalton Trans.* **2000**, 2801. (f) Jacobson, R. R.; Tyeklar, Z.; Farocq, A.; Karlin, K. D.; Liu, S.; Zubieta, J. *J. Am. Chem. Soc.* **1988**, *110*, 3690.

(27) (a) Sucha, V.; Sivak, M.; Tyrselova, J.; Marek; J. *Polyhedron* **1997**, *16*, 2837. (b) Bennett, M. J.; Donaldson, P. B. *Inorg. Chem.* **1977**, *16*, 1585.

Table 3. Selected Structural Parameters (Å, deg) for Peroxopalladium Complexes

				5	
param	**2b**	**3**	**4**	Pd1 part	Pd2 part
Pd−O	1.981(7)	1.988(4)	1.968(2)	1.993(6) (Pd1−O1)	
O−O	1.463(9)	1.436(5)	1.447(4)	1.439(8)	
O−X (X)		1.434(6) (C1)	1.968(2) (Pd1*)	1.968(5) (Pd2−O2)	
Pd−N[a]	2.100(6)	1.998(4)	2.060(2)	1.992(7) (Pd1−N11)	2.042(6) (Pd2−N51)
	2.057(9)	2.030(4)	2.023(2)	2.007(6) (Pd1−N21)	2.028(6) (Pd2−N61)
Pd−N[b]	3.07(1)	3.586(4)	3.485(2)	3.603(8) (Pd1−N31)	4.075(8) (Pd2−N71)
Pd−L (L)[c]	2.254(2) (P1)	2.023(4) (N41)	2.035(2) (N41)	2.027(6) (Pd1−N41)	2.044(5) (Pd2−O1)
Pd···Pd			4.6752(4)	3.6977(8)	
Pd−O−O	109.5(5)	114.2(3)	112.0(2)	119.0(4) (Pd1−O1−O2)	
O−O−X		109.4(3)	112.0(2)	71.8(3) (O1−O2−Pd2)	
Pd−O−O−X[d]		112.2(4)	180	127.1(4)	
N−Pd−N (κ^2-Tp^{iPr2})[a]	84.4(3)	87.2(2)	86.17(8)	85.2(2)	88.1(3)
N−Pd−O (trans)[a]	175.7(3)	174.5(2)	174.38(8)	167.8(3)	153.5(2) (O1−Pd2−N51)
N−Pd−O (cis)[a]	92.8(3)	87.8(2)	96.99(8)	94.8(2)	117.9(2) (O1−Pd2−N61)
O−Pd−L[c]	81.8(2)	96.1(2)	84.87(9)	88.4(2)	42.0(2) (O1−Pd2−O2)
Pd−O−Pd				132.7(3)	
N−Pd−L (trans)[a,c]	173.3(3) (P1)	174.8(2) (N41)	176.96(9)	176.1(2)	159.8(2) (O2−Pd2−N61)
N−Pd−L (cis)[a,c]	101.2(2)	89.0(2)	84.87(9)	91.2(2)	111.7(2) (O2−Pd2−N51)

[a] Parameters associated with the coordinated nitrogen atoms in the basal plane. [b] Parameters associated with the nitrogen atom in the pendant pz ring. [c] Parameters associated with the additional ligands, PPh_3 (**2b**), py (**3**−**5**), and μ-O_2 (**5**). [d] Dihedral angles.

Chart 3

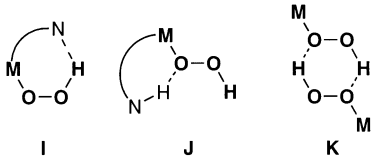

Scheme 4

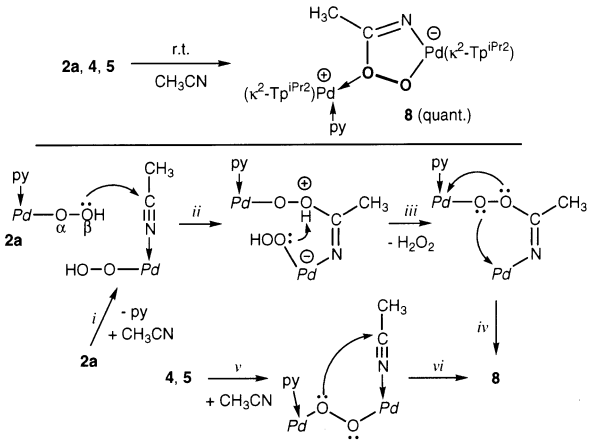

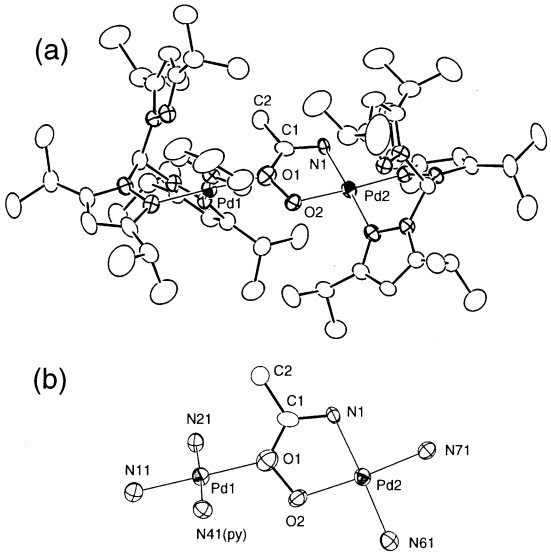

Figure 3. Molecular structures of **8** drawn with thermal ellipsoids at the 30% probability level: (a) overview; (b) expanded view of the core part.

stability toward moisture, mononuclear complexes **1**−**3** are not virtually affected, whereas dinuclear complexes **4** and **5** turn out to be so sensitive to moisture as to be readily hydrolyzed to a mixture containing **1** and **2a**.

The most characteristic reaction feature of the peroxopalladium complexes is their nucleophilic nature as typically exemplified by reaction with acetonitrile (Scheme 4). Dissolution of **2a**, **4**, and **5** in acetonitrile afforded pale yellow product **8**, whereas the *tert*-butylperoxo complex **3** was recovered even when heated at 50 °C. ^{1}H NMR monitoring of the reaction of **2a**, **4,** and **5** with CH_3CN in C_6D_6 revealed quantitative formation of **8**. A ^{1}H NMR spectrum of **8** containing two sets of Tp^{iPr2} signals indicates formation of an unsymmetrical dinuclear complex, and its cyclic structure is confirmed by X-ray crystallography. An ORTEP view is shown in Figure 3, and selected structural parameters are listed in Table 4. The O1−O2 distance [1.409(6) Å] falls in the range of single bond lengths, although it is slightly shorter than the O−O lengths in the starting compounds (∼1.45 Å; see above). The C1−N1 distance [1.305(8) Å] is comparable to C═N lengths, while the C1−O1 distance [1.333(8) Å] is between C−O and C═O lengths. These structural parameters are consistent with the zwitterionic 2,3-dioxa-5-azapalladacyclopent-4-ene structure, where the additional cationic Pd(Tp^{iPr2})(py) fragment is coordinated through the O1 atom. The structure of **8** is also supported by the $\nu_{C=N}$ vibration (1588 cm^{-1}) and FD-MS spectrum [m/z = 1296 (M$^+$)], and the square-planar coordination geometry resulting from the κ^2-coordination of the Tp^{iPr2} ligand is indicated by the ν_{BH} vibration (2476 cm^{-1}).[20] Although formation of peroxometallacycles from peroxometal species [(κ^2-O_2)ML$_n$] and electrophilic substrates such as ketone and quinone has precedents, in particular, for Pt−η^2-O_2 adducts,[19,28] complex **8** is

Table 4. Selected Structural Parameters for **8**[a]

Bond Lengths			
Pd1−O1	1.978(6)	Pd2−N51	2.004(6)
Pd1−N11	2.009(6)	Pd2−N61	2.006(4)
Pd1−N21	2.013(5)	Pd2−N71	3.949(5)
Pd1−N31	2.895(6)	O1−O2	1.409(6)
Pd1−N41	2.061(5)	O1−C1	1.333(8)
Pd2−O2	1.959(5)	N1−C1	1.305(8)
Pd2−N1	1.977(4)	Pd1···Pd2	4.6665(7)

Bond Lengths			
O1−Pd1−N11	177.0(2)	N1−Pd2−N61	177.0(2)
O1−Pd1−N21	91.2(2)	N51−Pd2−N61	89.3(2)
O1−Pd1−N41	90.8(2)	Pd2−N1−C1	110.4(3)
N11−Pd1−N21	86.0(2)	Pd1−O1−O2	115.3(3)
N11−Pd1−N41	92.1(2)	Pd1−O1−C1	130.3(4)
N21−Pd1−N41	177.0(2)	O2−O1−C1	113.9(5)
O2−Pd2−N1	82.7(2)	Pd2−O2−O1	111.1(3)
O2−Pd2−N51	175.7(2)	O1−C1−N1	121.9(5)
O2−Pd2−N61	94.6(2)	O1−C1−C2	120.3(6)
N1−Pd2−N51	93.3(2)	N1−C1−C2	117.8(5)

[a] Bond lengths in Å and bond angles in deg.

the first example of a peroxometallacyle formed from a (hydroperoxo)metal species.[29]

A possible reaction sequence for formation of **8** from **2a** is summarized in Scheme 4, which involves (i, ii) nucleophilic addition of the OOH ligand (at the β-oxygen atom) to the MeCN ligand activated through coordination at Pd, (iii) deprotonation by the action of the hydroperoxo ligand, and (iv) coordination of the α-peroxo oxygen atom associated with 1,2-migration of the (Tp^{iPr2})(py)Pd fragment on the peroxo linkage. The peroxometallacycle **8** could be also formed from the dinuclear complexes **4** and **5** via (v) coordination of MeCN at a Tp^{iPr2}Pd moiety followed by (vi) nucleophilic addition. Although the *tert*-butylperoxo complex **3** shows structural features similar to those of **2a** as mentioned above, steric hindrance of the nucleophilic addition by the bulky *tert*-butyl group (step ii) and difficulty in the C−O bond cleavage (removal of the *tert*-butyl group; analogous to step iii) are possible reasons for the lack of reactivity of **3** toward CH_3CN. At the moment, however, we have no evidence to eliminate the possibility of the initial reaction at the proximal oxygen atom of the OOH moiety.

The reactivity of (hydroperoxo)metal species has been interpreted in terms of the processes associated with the proximal α oxygen atom (e.g. insertion into or cleavage of the M−O_α or O−O bond), because M−OOH species have been regarded as analogues of the more extensively studied M−OOR species. But the proposed mechanism (Scheme 4) suggests that not only the proximal α oxygen atom but also the distal β oxygen atom of M−OOH species can be the nucleophilic reaction site.

Such a nucleophilic character is also exemplified by the oxygenation reaction of acetaldehyde leading to quantitative

Scheme 5

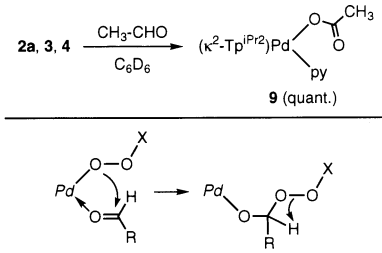

Scheme 6

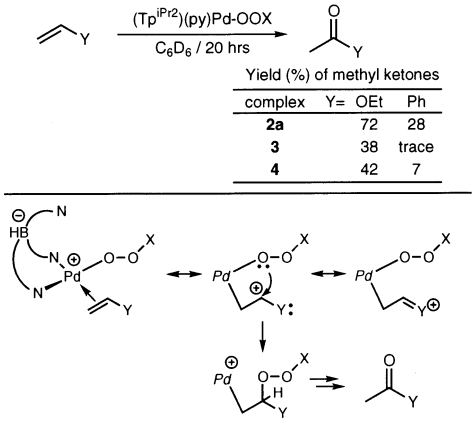

conversion to the acetato complex **9**[11] (Scheme 5).[30] Nucleophilic attack of the peroxo moiety at the α-carbon atom of the coordinated aldehyde molecule should be involved in the formation of **9**.

Although the peroxopalladium complexes **2a**, **3,** and **4** exhibited oxygenation activity toward polar (electrophilic) substrates, they turned out to be sluggish with respect to oxygenation of less polar substrates. For example, treatment with PPh_3 resulted in the formation of O=PPh_3 in moderate yields at ambient temperature [yields of O=PPh_3: 71% (**2a**; 1.5 h); 43% (**3**; 5 h); 45% (**4**; 5 h)], but it should be noted that a part of **2a** was converted to the PPh_3-substituted complex **2b** (see above) indicating occurrence of concomitant oxygenation and ligand substitution. We also examined oxygenation of unsaturated hydrocarbons. While nonfunctionalized alkene such as 1-hexene was left unaffected, oxidative conversion of vinyl groups into methyl ketones was observed for ethyl vinyl ether and styrene in low to moderate yields (Scheme 6; yields determined by GLC analyses). No epoxidation was observed, and the inorganic products very soluble in organic solvents could not be isolated nor identified. Although the reaction mechanism is not clear at the present time, the ketonization should be initiated by coordination of the electron-donating olefinic substrate to the Pd center, which bears cationic character to compensate the negative charge at the anionic borate part. Subsequent migration of the OOX moiety followed by H-abstraction by the OX group (see Scheme 5) or β-hydrogen elimination would finally produce methyl ketone. The low reactivity of the Tp^{iPr2}Pd−peroxo complexes compared to

(28) Valentine, J. S. *Chem. Rev.* **1973**, *73*, 235. Dieck, H. T.; Fendesak, G.; Munz, C. *Polyhedron* **1991**, *10*, 255. Pizzotti, M.; Cenini, S.; Ugo, R.; Demartin, F. *J. Chem. Soc., Dalton Trans.* **1991**, 65.

(29) Formation of a peroxocarbonate complex from a peroxo species was reported recently: Hashimoto, K.; Nagatomo, S.; Fujinami, S.; Furutachi, H.; Ogo, S.; Suzuki, M.; Uehara, A.; Maeda, Y.; Watanabe, Y.; Kitagawa, T. *Angew. Chem., Int. Ed.* **2002**, *41*, 1202.

(30) Because slow decomposition was evident for complex **5** upon dissolution in organic solvents, reactivity was studied for **2a**, **3**, and **4**.

previously reported group 8 metal peroxo complexes such as those reported by Strukul et al.[3f,19h,31] could be partly ascribed to the steric congestion around the metal center. For example, a cyclic β-hydroperoxoalkyl intermediate with the distal hydroperoxo oxygen atom being coordinated to the metal center was proposed for catalytic epoxidation of alkenes. In the Tp^{iPr2}Pd systems initial olefin coordination should be hindered by the pz^{iPr2} groups bearing rather bulky isopropyl groups, and O-coordination of the β-hydroperoxoalkyl group may be hindered by the pendant pz^{iPr2} ring as well as by hydrogen-bonding interaction with it. Another different key feature is the type of the central metal and supporting ligand, P- vs N-donors, but definite conclusion cannot be obtained on the basis of the structural features and chemical properties of our complexes revealed so far alone.

Conclusions

A series of (hydroperoxo)-, (alkylperoxo)-, and (μ-peroxo)-palladium complexes bearing the (Tp^{iPr2})(L)Pd auxiliary **2**−**5** has been prepared and fully characterized by spectroscopic and crystallographic methods. Typical features of the present (Tp^{iPr2})(L)Pd−OOX system are as follows: (1) The present system reveals the effectiveness of the dehydrative condensation method for the selective synthesis of peroxometal species. (2) The structural parameters associated with the O−O moieties are consistent with the description of the O−O parts as "peroxide". (3) The isolated peroxopalladium complexes turn out to be thermally stable, although the coordinated pyridine ligand is found to be kinetically labile. (4) The peroxo moieties are nucleophilic enough to add across the C≡N or C═O bonds in polar organic substrates.

Application of the dehydrative condensation to other systems is now under study, and results will be reported in due course.

Acknowledgment. We are grateful to the Ministry of Education, Culture, Sports, Science, and Technology of the Japanese Government for financial support of this research (Grant-in-Aid for Scientific Research for Priority Areas 11228201). We thank Professor Akihide Wada of our Laboratory for the measurements of Raman spectra.

Supporting Information Available: Tables for positional parameters and B_{eq} values, anisotropic thermal parameters, and interatomic distances and bond angles, ORTEP structures, and CIF files. This material is available free of charge via the Internet at http://pubs.acs.org.

IC020355E

(31) Strukul, G.; Michelin, R. A. *J. Am. Chem. Soc.* **1985**, *107*, 7563.